Available online at www.sciencedirect.com

ScienceDirect

Journal of Hydro-environment Research ■■ (2016) ■■–■■

Journal of Hydro-environment Research

www.elsevier.com/locate/jher

Research papers

# Comparison of different statistical downscaling methods for climate change rainfall projections over the Lake Victoria basin considering CMIP3 and CMIP5

C. Onyutha [a,b,*], H. Tabari [a], A. Rutkowska [c], P. Nyeko-Ogiramoi [d], P. Willems [a,e]

[a] Hydraulics Laboratory, Katholieke Universiteit Leuven, Kasteelpark Arenberg 40, Leuven B-3001, Belgium
[b] Faculty of Technoscience, Muni University, P.O Box 725, Arua, Uganda
[c] Department of Applied Mathematics, University of Agriculture, Kraków, Poland
[d] Rural Water and Sanitation Department, Ministry of Water and Environment, 22/28 Port Bell Road, Luzira, P.O Box 200026, Kampala, Uganda
[e] Department of Hydrology and Hydraulic Engineering, Vrije Universiteit Brussel, Pleinlaan 2, 1050 Elsene, Brussel, Belgium

Received 18 January 2015; revised 7 January 2016; accepted 1 March 2016

Available online

**Abstract**

In this study, outputs of three statistical downscaling (SD) methods including the change factor (Delta), simplified (simQP) and advanced (wetQP) quantile-perturbation-based approaches were compared based on daily rainfall series at 9 meteorological stations in the Lake Victoria basin (LVB) in Eastern Africa. The comparison was made considering phase 5 and phase 3 of the Coupled Model Inter-comparison Project, i.e. CMIP5 and CMIP3 respectively. For the CMIP5 (CMIP3) at each station, there were a total of 7 (14) GCMs, 18 (20) daily historical (control) simulations over the period 1961–2000, and 35 (49) daily future projection series of the periods 2050s and 2090s. The ensemble mean of the GCMs' *Bias* in reproducing rainfall extremes for return periods in the range of 1 to 40 years for the CMIP5 (CMIP3) varied from −19.05% to 3.11% (−65.85% to −4.86%). For the high greenhouse gas scenario rcp8.5 (A2) of the CMIP5 (CMIP3), the ensemble mean of the projected changes over the LVB in the 10-year rainfall intensity quantile obtained from the Delta, simQP, wetQP SD goes up to 5.8, 10 and 22.4% (11.7, 15.9 and 43.6%) in the 2050s and 8, 11.4, and 25.4% (14.2, 23.3 and 40.6%) in the 2090s. Rainfall totals of the main wet (dry) season are generally projected to increase (decrease) in both the 2050s and 2090s. Because the outputs from the three SD methods captured well the pattern of monthly rainfall totals, the difference between the projected changes of seasonal or annual rainfall totals from the Delta, simQP and wetQP was shown to be insignificant. However, the differences in the results from the Delta, simQP and wetQP methods with respect to the projections of rainfall quantiles indicate that the choice of the SD method can be made on a case by case basis in line with the objectives of the climate change impact study, e.g. the Delta does not capture well the changes in rainfall extremes, whereas the wetQP is suitable for both rainfall extremes and rainfall totals at both seasonal and annual time scales. The findings of this study also show the need to consider evaluations of the inter-GCM differences in the LVB as a data scarce region in assessing the discernible impact of climate change on rainfall extremes and/totals for decision making related to water resources management and engineering.


*Keywords:* Climate change; Statistical downscaling; GCMs; CMIP3 versus CMIP5; Rainfall; Lake Victoria basin

## 1. Introduction

Planning, design and operation of a number of water engineering applications including water supply projects (e.g. dikes, dams, irrigation systems) or urban drainage facilities such as sewer conduits, etc., require statistics of rainfall intensity quantiles and/or totals. The challenge that the contemporary water managers are faced with in their decision making is debatably the impact of climate change on the hydrometeorology. The hypothesized impact of global warming has seized an immense portion of the international attention directed toward investigating the effect of climate change on water resources. Examples of some recent climate change impact studies include Artlert et al. (2013), Fathelrahman et al. (2014), Lee et al. (2014), and Nkomozepi and Chung (2014). Changes in rainfall is a critical factor, among other hydro-climatological variables, to determine the influence of the climate system on hydrology in support of water resources

* Corresponding author. Hydraulics Laboratory, Katholieke Universiteit Leuven, Kasteelpark Arenberg 40, Leuven B-3001, Belgium.
*E-mail address:* charles.onyutha@bwk.kuleuven.be (C. Onyutha)

http://dx.doi.org/10.1016/j.jher.2016.03.001
1570-6443/

management in a regional attempt to adapt to climate change impacts. Changes in climate extremes and their impacts on the natural physical environment were examined by the Intergovernmental Panel on Climate Change, IPCC (2012). The need to consider changes in climate conditions was also emphasized in the fifth Assessment Report (AR5) of the IPCC (2013).

A number of studies have shown that climate change will have a considerable impact on the water resources. This is also the case for the Nile basin (which has its key source of drainage from the Lake Victoria basin (LVB)) as shown by, among others, Beyene et al. (2010), Conway and Hulme (1996), Githui et al. (2009), Nyeko-Ogiramoi et al. (2010), Taye et al. (2011), and Tungaraz et al. (2012). Many of the above cited references show significant bias in the General Circulation Models (GCM) results of the Coupled Model Inter-comparison Project (CMIP), especially of the previous generation, i.e. phase 3 (CMIP3). However, due to improvements in the GCMs, a reduction in their bias was expected in the recently released phase 5 (CMIP5). The performance of the GCMs from the CMIP5 to reproduce the rainfall over the Lake Victoria was recently assessed by Akurut et al. (2014). Such study (with limited focus rather on the Lake Victoria than the entire basin, i.e. LVB) is, with respect to the lake outflow, important for hydropower operations and planning, e.g. for Owen Falls Dam, and abstraction, say, for irrigation. Considering the entire LVB as done in this study is vital for agricultural practices and risk-based water engineering management. Despite the need for climate change impact assessment in the study area, the issue of data quality as reflected in the uncertainty analyses (see e.g. Kizza et al., 2011; Onyutha and Willems, 2013; Onyutha and Willems, 2015a) cannot be ignored despite some remedial attempts to deal with it, for instance by Nyeko-Ogiramoi et al. (2012a), Kizza et al. (2013) and Onyutha and Willems (2015b). Questionable data quality is one reason for the bias in the GCMs to reproduce rainfall. This, with respect to rainfall intensity extremes and totals, highlights the need for an insight into amount by which the GCMs of the CMIP5 were improved compared with those of the CMIP3 to capture the typical conditions of data scarcity and/or questionable data quality of the LVB. Although comparison between the CMIP3 and CMIP5 for rainfall projections was recently made on a global scale by Kumar et al. (2014), by the time of this study, no such attempts at the level of catchment or basin especially for the study area could be found in literature.

Because significant bias in the GCM results may be valid as well for the future projections, it makes them inappropriate for direct use in climate change impact assessment at local scale. Eventually, downscaling and/or bias correction is first required before impact analysis of climate change is done. Despite the general assumption that the major sources of uncertainty are linked to the GCMs and Greenhouse Gases Emissions Scenarios (GGES) (Chen et al., 2011), other sources exist such as the statistical method applied to transfer the climate change signal obtained from the GCM results to the local, case-specific impacts. This transfer is commonly done using the statistical downscaling (SD). The influence of the SD methods on climate change impact analysis was investigated before by Chen et al. (2011), Ghosh and Katkar (2012), Khan et al. (2006), Prudhomme and Davies (2009), Quintana-Segui et al. (2010), etc. Some studies, e.g. Prudhomme and Davies (2009), demonstrated that uncertainties from GCMs are larger than those from the downscaling methods and GGES. In the impact assessment of climate change on rainfall extremes in the LVB, the uncertainties stemming from the inter-GCM differences, and those due to the choice of the SD method cannot be ignored. The main SD methods used to project climate changes on hydro-meteorological variables in the study area include the change factor (Delta) and quantile-based perturbation approaches. Just to mention some few examples for the LVB, the Delta method was used by Dessu and Melesse (2013), and the quantile-based SD was applied by Akurut et al. (2014), and Nyeko-Ogiramoi et al. (2012b). According to Melesse et al. (2011), one of the main causes of food insecurity and the most daunting challenge the entire Nile Basin (where LVB is located) faces is the subsistence and rain-fed agriculture, together with high rainfall variability. This problem in the LVB is exacerbated by severe damage to public life and property inflicted by extreme rainfalls and associated flooding events, for instance, downstream of Nzoia River and Nyando River, and around the Budalang'i and Kano plains. These altogether mean that for appropriate regional planning of adaptation measures for the climate change impacts with respect to agriculture and risk-based water management, it is important to consider both seasonal or annual rainfall volumes and the extreme events. It is known, as will also be shown in this study that, the Delta method is suitable for changes in the mean of rainfall, and the quantile-based perturbation approach is commendable for extreme events. However, in each of the previous climate change studies for the LVB, projections of rainfall were made either based on only the Delta method (Dessu and Melesse, 2013) or the quantile-based perturbation approach (Akurut et al., 2014; Nyeko-Ogiramoi et al., 2012b) but not using both methods. In this study, both SD methods were used to provide findings to incorporate impacts of climate change in both agricultural practices and risk-based water management. The difference, if any, among the SD methods indicate the need to assess influence due to the choice of the particular downscaling approach on the projections of the hydro-meteorological variables.

This study, therefore with respect to the insights into the uncertainty in the climate change projections of rainfalls across the LVB, is aimed at: 1) assessing the influence of the SD methods on the projections of rainfall extremes as well as annual and seasonal totals, and 2) comparatively performing consistency check of the CMIP3 and CMIP5 GCMs in reproducing historical conditions of rainfall extremes and totals.

## 2. Study area and data series

### 2.1. Study area

The LVB, which has a total catchment area of about 184,000 km$^2$, stretches 355 km in east–west direction (31°37′E to 34°53′E) and 412 km in north–south direction (00°30' N to 3°12′S). It comprises Lake Victoria which is the largest freshwater body in Africa and the second largest in the world. Lake Victoria, which has a shoreline of 4828 km and a surface area of

Please cite this article in press as: C. Onyutha, H. Tabari, A. Rutkowska, P. Nyeko-Ogiramoi, P. Willems, Comparison of different statistical downscaling methods for climate change rainfall projections over the Lake Victoria basin considering CMIP3 and CMIP5, Journal of Hydro-environment Research (2016), doi: 10.1016/j.jher.2016.03.001

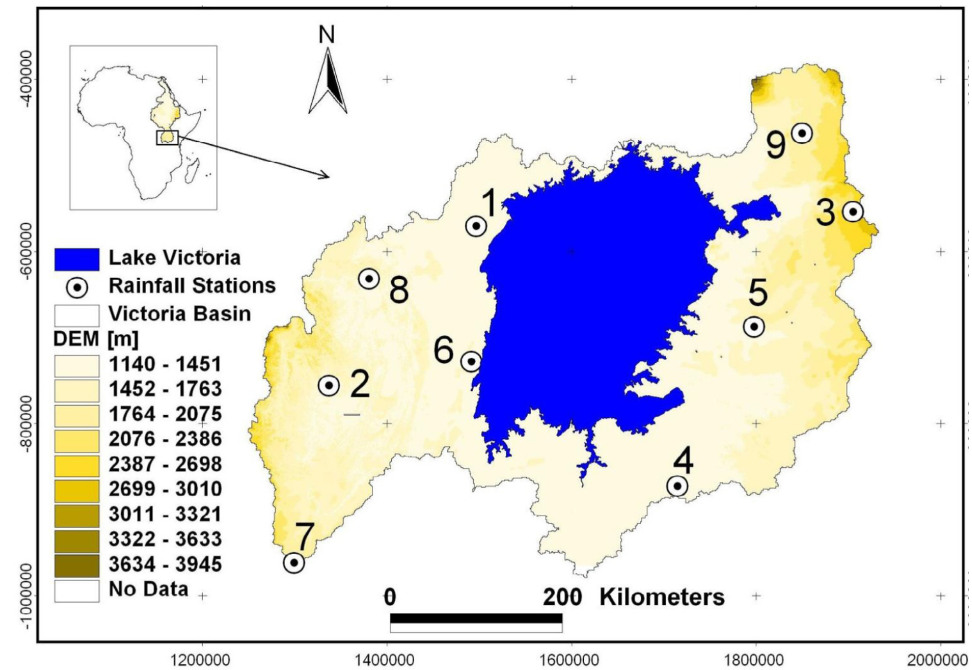


Fig. 1. Locations of the meteorological stations (see Table 1 for details). The background map is based on the Digital Elevation Model (DEM) obtained online from the International Centre for Tropical Agriculture, CIAT-CSI SRTM website, http://strm.csi.cgiar.org/ [accessed 30th November, 2010]. The longitudes and latitudes are in kilometers.

68,800 km$^2$, is situated at an altitude of 1134 m above sea level. It has a relatively small drainage basin, slightly less than three times the lake's surface in area (Fig. 1). According to Awange and Ong'ang'a (2006), the climate of the LVB is generally tropical humid, with temperatures ranging from 15°C in the highlands, to 28°C in the semi-arid areas. The mean annual rainfall in the LVB varies from about 886 mm to 2600 mm. Albeit Lake Victoria is geopolitically shared by Kenya, Uganda and Tanzania in the proportion of 6%, 43% and 51% respectively (Awange and Ong'ang'a, 2006), the LVB stretches over five countries including also Burundi and Rwanda. The details on the stations are shown next.

## 2.2. Observed rainfall

Daily observed rainfall data (for the period 1961–2000) of 9 selected meteorological stations (Table 1) distributed in the LVB (Fig. 1) were obtained from the database of the FRIEND/Nile (River Nile basin Flow Regimes from International, Experimental and Network Data) project (United Nations Educational Scientific & Cultural Organization (UNESCO, 2014). Since these datasets are similar to those used by Onyutha and Willems (2015a), the details of the comparison between the series from the stations, in-filling of the missing rainfall data using the inverse distance weighted interpolation technique, other procedures for the data quality control and analysis can be obtained from the cited reference. The coefficient of skewness (actual excess kurtosis) of the daily rainfall at the selected locations and data periods was noted to vary in the range 2.9 (12.0) at station 2 to 5.4 (42.3) at station 4. Similarly, the coefficient of variation ranges from 1.4 (station 2) to 3.1 (station 4). This shows a considerable variability on a day to day basis in the LVB (Onyutha and Willems, 2015a).

Table 1
Overview of selected stations.

| Number | Station ID | Station name | Longitude [°] | Latitude [°] | Mean [mm/day] |
|---|---|---|---|---|---|
| 1 | 9031026 | Kamenyamigo | 31.67 | −0.30 | 2.6 |
| 2 | 70009 | Kigali Aero Nyabarongo | 30.13 | −1.97 | 6.6 |
| 3 | 9035002 | Londiani Forest | 35.60 | −0.15 | 3.2 |
| 4 | 9333005 | Maswa Hydromet | 33.77 | −3.17 | 2.5 |
| 5 | 9134008 | Nyabassi | 34.57 | −1.35 | 3.9 |
| 6 | 9131001 | Rubya Mission | 31.62 | −1.72 | 3.8 |
| 7 | 10161 | Ruvyironza | 29.77 | −3.82 | 3.6 |
| 8 | 9030012 | Rwoho Forest | 30.55 | −0.85 | 2.6 |
| 9 | 8935076 | Turbo Forest | 35.02 | 0.67 | 3.6 |

Source: Onyutha and Willems (2015a).



Please cite this article in press as: C. Onyutha, H. Tabari, A. Rutkowska, P. Nyeko-Ogiramoi, P. Willems, Comparison of different statistical downscaling methods for climate change rainfall projections over the Lake Victoria basin considering CMIP3 and CMIP5, Journal of Hydro-environment Research (2016), doi: 10.1016/j.jher.2016.03.001

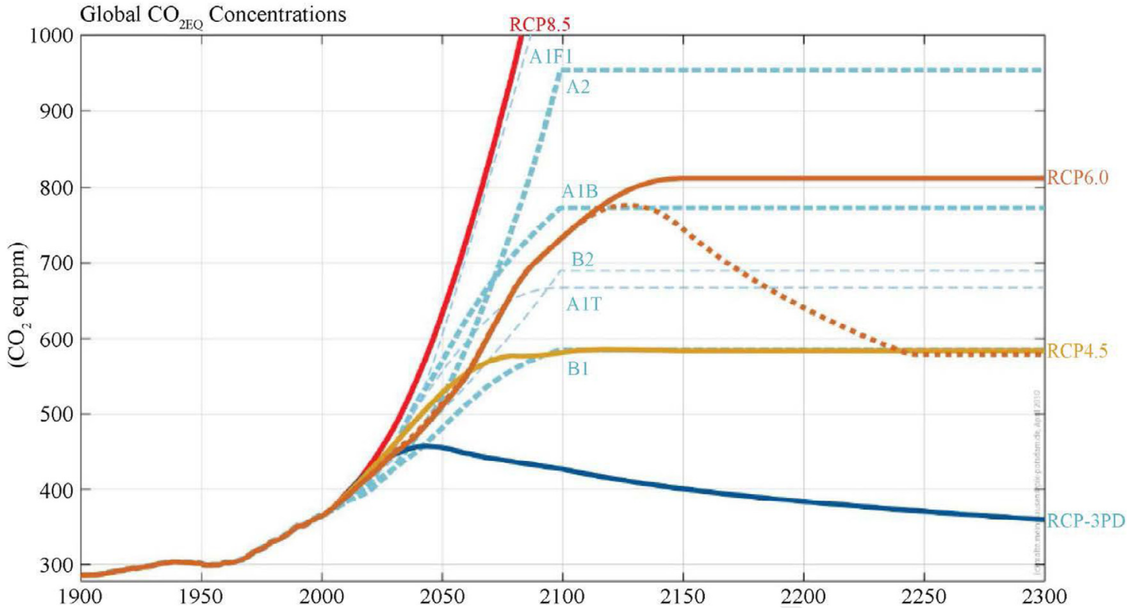


Fig. 2. Comparison of the scenarios for CMIP3 and CMIP5. (Source: IPCC, 2013).

### 2.3. Global climate models

According to the Data Distribution Center DDC (2015) of the IPCC, GCMs are the most advanced tools currently available for simulating the response of the global climate system to increasing greenhouse gas concentrations. The GCMs, representing physical processes in the atmosphere, ocean, cryosphere and land surface, depict the climate using a three dimensional grid over the globe typically having 10 to 20 vertical layers in the atmosphere (as many as 30 layers in the oceans) and a horizontal resolution of between 250 and 600 km (DDC, 2015). Important to note is that the GCMs are quite coarse compared to the scales used for impact assessments. The sources of uncertainty in the GCMs include: lack of proper modelling of some physical processes such as those related to clouds at smaller scales, simulation of different responses due to various feedback mechanisms for instance water vapor and warming, clouds and radiation, ocean circulation and ice and snow albedo.

In this study, two sets of global climate model simulations were used, i.e. CMIP3 (Meehl et al., 2007) and CMIP5 (Taylor et al., 2012) which were the basis of the fourth and fifth IPCC assessment reports, respectively. Whereas the IPCC GGES was used in the CMIP3, the CMIP5 considered the Representative Concentration Pathways (RCP). The IPCC special report emission scenarios SRES of the CMIP3 include B1, B2, A1B, A1F1, A1T, and A2. These SRES (which are detailed socio-economic pathways), with respect to the storylines (Nakicenovic et al., 2000), may be taken to characterize a world more: integrated (A1), divided (A2), integrated and ecologically friendly (B1), and divided but ecologically friendly (B2). On the other hand, the scenarios of the CMIP5 are the RCPs 2.6, 4.5, 6.0, and 8.5. The RCP2.6 is also called the RCP-3PD, and PD stands for Peak and Decline. The numbers after 'RCP' denote the global energy imbalances (radiative forcings) in watts per square meter by the year 2100. Because the scenarios in the CMIP3 and CMIP5 are different, a direct comparison of hydrometeorological projections from the two datasets in a meaningful way is impossible. The relationship between the SRES (of CMIP3) and the RCPs (of CMIP5) with respect to carbon dioxide ($CO_2$) concentration is shown in Fig. 2. According to Knutti and Sedlácek (2012), the efforts for CMIP5, compared with those of the CMIP3, are enormous, with a larger number of more complex models run at higher resolution, with more complete representations of external forcings, more types of scenario and more diagnostics stored.

For the CMIP3, the daily rainfall time series of 14 GCMs (Table 2) were obtained from the Program for Climate Model Diagnosis and Inter-comparison (PCMDI) database. These 14 GCMs were selected because their robustness to reproduce rainfall extremes and totals for the study area was demonstrated by Nyeko-Ogiramoi et al. (2012b). The archived daily data in the PCMDI database (last accessed online at http://www2-pcmdi.llnl.gov/esg_data_portal on 08 June 2011) for control simulations are for the period 1961–2000 and for future projections are for 2046–2065 (2050s) and 2081–2100 (2090s). According to IPCC (2001), a 30-year period is sufficient to assess the climate change. However, due to the challenges in climate modelling and archiving of the global climate data especially for the CMIP3, the scientific fraternity was forced to consider a 20-year period for plausible climate change impact assessment (Nyeko-Ogiramoi et al., 2012b). According to Nyeko-Ogiramoi et al. (2012b), the deviation of the climate change projection based on the 20-year future scenario is not significantly different from that of the 30-year period.

For the CMIP5, data of 7 GCMs (Table 2) were obtained from the PCMDI database (last accessed online at http://cmip-pcmdi.llnl.gov/cmip5/data_portal.html on 03

Please cite this article in press as: C. Onyutha, H. Tabari, A. Rutkowska, P. Nyeko-Ogiramoi, P. Willems, Comparison of different statistical downscaling methods for climate change rainfall projections over the Lake Victoria basin considering CMIP3 and CMIP5, Journal of Hydro-environment Research (2016), doi: 10.1016/j.jher.2016.03.001

Table 2
Overview of GCM runs used in the study.

| Model identity | | | | | |
|---|---|---|---|---|---|
| In this paper | According to the IPCC | Runs (R) | | | |
| CMIP3 | | Ctrl | A1B | B1 | A2 |
| AOM | GISS-AOM | 1 | 1 | 1 | |
| BCM2.0 | BCCR-BCM2.0 | 1 | 1 | 1 | 1 |
| CGT47 | CGCM3.1(T47) | 1–3 | 1–3 | 1–3 | 1–3 |
| CGT63 | CGCM3.1(T63) | 1 | 1 | 1 | |
| CM2.0 | GFDL-CM2.0 | 1 | 1 | 1 | 1 |
| CM2.1 | GFDL-CM2.1 | 1 | 1 | 1 | 1 |
| CM3.0 | INM-CM3.0 | 1 | 1 | 1 | 1 |
| ECH4 | MPI- ECHAM4-OM | 1 | 1 | | 1 |
| ECH5 | ECHAM5/MPI-OM | 1,4 | | 1 | 1 |
| ECHO-G | ECHO-G | 1–3 | 2–3 | 1–3 | 1–3 |
| MI3.2H | MIROC3.2(hires) | 1 | 1 | 1 | 1 |
| MI3.2M | MIROC3.2(medres) | 1–2 | 2 | 2 | 2 |
| MK3.0 | CSIRO-MK3.0 | 1 | 1 | 1 | 1 |
| MK3.5 | CSIRO-MK3.5a | 1 | 1 | 1 | 1 |
| CMIP5 | | His. | rcp4.5 | rcp6.0 | rcp8.5 |
| BNU | BNU_ESM | 1 | 1 | | 1 |
| MK3.6 | CSIRO-Mk3-6-0 | 1–10 | 1–10 | 1–10 | 10 |
| FG2 | FGOALS-g2 | 1 | 1 | | 1 |
| GFCM | GFDL-CM3 | 1,3 | 1,3 | 1 | 1 |
| GESM | GFDL-ESM2G | 1 | 1 | 1 | |
| MLR | MPI-ESM-LR | 1 | 1 | | 1 |
| MMR | MPI-ESM-MR | 1 | 1 | | 1 |

Ctrl (His.): CMIP3 (CMIP5) control (historical) simulation; A1B, B1 and A2: CMIP3 scenarios and, rcp4.5, rcp6.0 and rcp8.5: CMIP5 scenarios.

Table 3
Institutions of the GCMs used in the study.

| Country | IPCC model identity | Institution |
|---|---|---|
| CMIP3 | | |
| USA | GISS-AOM | NASA/Goddard Institute for Space Studies |
| Norway | BCCR-BCM2.0 | Bjerknes Centre for Climate Research |
| Canada | CGCM3.1(T47)<br>CGCM3.1(T63) | Canadian Centre for Climate Modelling & Analysis |
| USA | GFDL-CM2.0<br>GFDL-CM2.1 | US Dept. of Commerce / NOAA / Geophysical Fluid Dynamics Laboratory |
| Russia | INM-CM3.0 | Institute for Numerical Mathematics |
| Germany | MPI- ECHAM4-OM<br>ECHAM5/MPI-OM | Max Planck Institute for Meteorology |
| Germany/Russia | ECHO-G | Meteorological Institute of the University of Bonn, Meteorological Research Institute of KMA, and Model and Data group. |
| Japan | MIROC3.2(hires)<br>MIROC3.2(medres) | Center for Climate System Research (The University of Tokyo), National Institute for Environmental Studies, and Frontier Research Center for Global Change (JAMSTEC) |
| Australia | CSIRO-MK3.0<br>CSIRO-MK3.5a | CSIRO Atmospheric Research |
| CMIP5 | | |
| China | BNU_ESM | College of Global Change and Earth System Science, Beijing Normal University |
| Australia | CSIRO-Mk3-6-0 | Commonwealth Scientific and Industrial Research Organisation in collaboration with the Queensland Climate Change Centre of Excellence |
| China | FGOALS-g2 | LASG, Institute of Atmospheric Physics, Chinese Academy of Sciences; and CESS, Tsinghua University |
| USA | GFDL-CM3<br>GFDL-ESM2G | Geophysical Fluid Dynamics Laboratory |
| Germany | MPI-ESM-LR<br>MPI-ESM-MR | Max Planck Institute for Meteorology (MPI-M) |

March 2014). For plausible comparison of results from both phases of the CMIP, the CMIP5 data over the same periods as those of the CMIP3 were considered. There were a total of 20 (18) control (historical) simulations and 49 (35) future projections for the CMIP3 (CMIP5). Three GGES (i.e. A2, A1B and B1) and RCPs (i.e. rcp8.5, rcp6.0 and rcp4.5) of the CMIP3 and CMIP5, respectively were used. To obtain an insight into the climate projections in a representative way, a GCM from the CMIP5 was selected if it had data available for the historical simulation and at least two of the three future scenario runs (i.e. rcp4.5, rcp6.0 and rcp8.5). More information on the institutions for the GCMs used in this study is provided in Table 3.

## 3. Methodology

### 3.1. *Inter-comparison and evaluation of the GCMs' performance*

Prior to the inter-comparison and performance evaluation, scaling of the observed gauge (or point) to areal rainfall was done using the areal reduction factors provided for the study area by Fiddes et al. (1974). This up-scaling of point to grid rainfall accounts for the expected systematic difference between the observed point rainfall and the grid averaged GCM rainfall. The inter-comparison and evaluation of the GCMs' performance were made with respect to the quantile/frequency analysis, and the ability to reproduce the seasonal and annual rainfall totals.

In line with frequency analysis, the data are required to be independent and identically distributed. One way to achieve this is through extraction from the full series of Annual Maxima Series (AMS). In the AMS, the time slice is chosen to be one hydrological year, and extremes with strong independence can be obtained. This is why the traditional AMS approach is still the most used method in flood frequency analysis in many countries of the world (Bezak et al., 2014), and hence adopted in this study. Considering $i$ as the rank of the AMS extracted extreme events ($i = 1$ for the highest) and $R$ the data record length in years, the empirical exceedance frequency or return period $T$ was calculated as the ratio of $R$ to $(i + 1)$.

For the comparison of rainfall totals, monthly, seasonal and annual time scales were considered. For each year, the rainfall total at the relevant time scale was obtained. In the next step, the average for the totals from the different years was calculated. Based on the known bimodal rainfall pattern of the equatorial

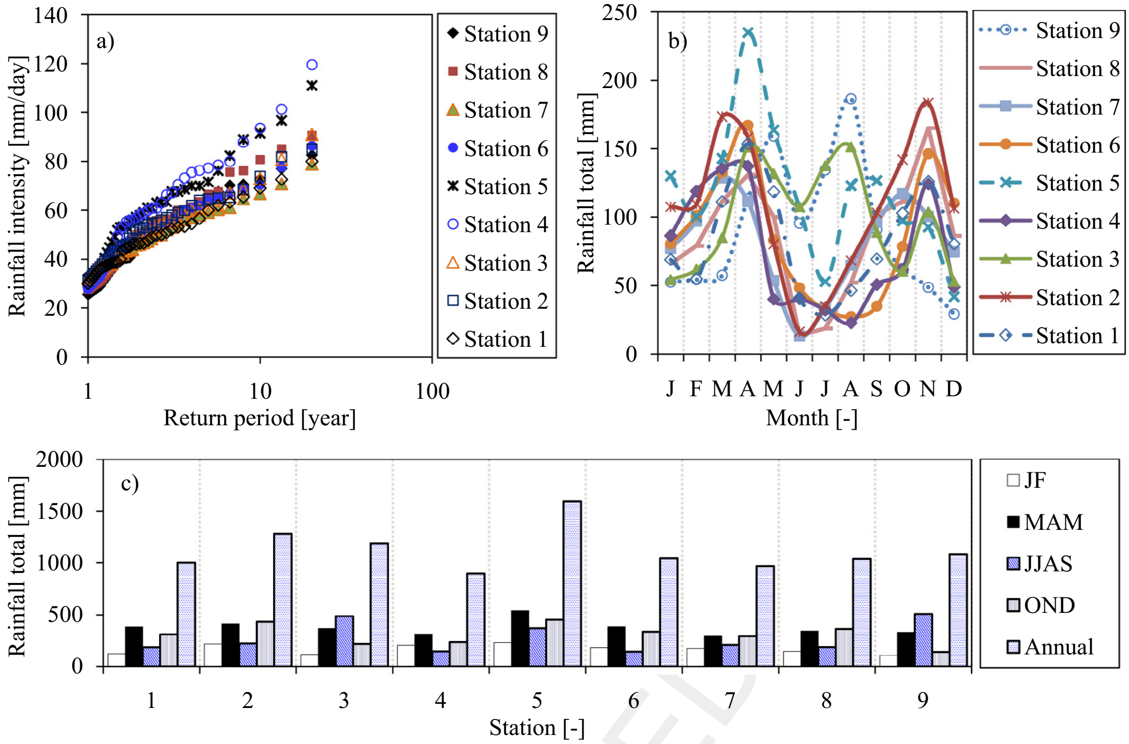


Fig. 3. (a) Daily rainfall intensity quantiles versus empirical return period, and rainfall totals for (b) monthly, and (c) seasonal and annual time scales.

region, i.e. with two wet and dry seasons (Nicholson, 1996), the seasonal totals were obtained over the months of January to February (JF), March to May (MAM), July to September (JJAS), and October to December (OND). For the north eastern quadrant (NEQ) of the LVB (stations 3 and 9), the July to September (JJAS) period is a wet season. For the remaining parts of the LVB, the main (short) dry season falls in the JJAS (JF). The main (short) wet season is in the MAM (OND).

The annual total for each year was obtained by summing up the rainfall depths over all the months from January to December. The seasonal and annual rainfall totals were obtained for both the observed and GCM-based daily series. This was done for both the CMIP3 and CMIP5.

For the different stations, examples of the observed AMS rainfall quantiles versus empirical Ts, and totals at different time scales are shown in Fig. 3a–c respectively.

The empirical Ts were graphically compared, for both the CMIP3 and CMIP5, with those from the rainfall annual maxima of the GCMs. Considering $n$ as the sample size of the annual maxima covering the Ts from 1 to 40 years, statistically the average of the difference between the GCM-based ($x_g$) and the empirical ($x_e$) quantiles of rainfall intensity as a percentage of $x_g$ was computed and hereafter called *Bias* [%] (Eq. 1). The root mean squared differences between $x_e$ and $x_g$ was also evaluated, hereafter denoted as *SEE* (standard error of the estimate) (Eq. 2). A good GCM would have its bias and *SEE* both close to zero.

$$Bias[\%] = \frac{1}{n}\sum_{i=1}^{n}\left(\frac{x_{g,i} - x_{e,i}}{x_{g,i}} \times 100\right) \quad (1)$$

$$SEE[mm/day] = \left(\frac{1}{n}\sum_{i=1}^{n}\left(x_{g,i} - x_{e,i}\right)^2\right)^{0.5} \quad (2)$$

The ability of the GCMs to capture the pattern of monthly rainfall totals (Fig. 3b) was also examined for both the CMIP3 and CMIP5.

### 3.2. Comparison of downscaling methods

Downscaling can be done through either statistical (empirical) methods conditioned on large-scale predictors or dynamical through the use of a regional climate model with the GCM outputs as the boundary condition. The tendency of the dynamic downscaling to be computationally intensive makes its application highly limited in the case where different GCMs with multiple GGES are considered in multi-decade simulations. Eventually, the SD methods as adopted in this study are more widely used because they require less computation time than those of the dynamical downscaling. The change factor (Delta) method is the simplest SD technique, which applies climate model-scale projections in the form of change (or perturbation) factors as seen in Prudhomme et al. (2002). Other SD methods include regression models, resampling methods based on weather typing schemes and stochastic weather generators. A review on statistical and dynamical downscaling methods can be found in Fowler et al. (2007) and Maraun et al. (2010).

In this study, the Delta approach was applied in its simple and advanced forms. The advanced forms selected are the quantile perturbation techniques because of the specific focus on downscaling extreme rainfall quantiles of the study area. By



Please cite this article in press as: C. Onyutha, H. Tabari, A. Rutkowska, P. Nyeko-Ogiramoi, P. Willems, Comparison of different statistical downscaling methods for climate change rainfall projections over the Lake Victoria basin considering CMIP3 and CMIP5, Journal of Hydro-environment Research (2016), doi: 10.1016/j.jher.2016.03.001

assuming that the bias in the GCM control simulations is similar to that of scenario runs, the climate change signals in terms of the quantile perturbation factors are considered bias-free. The SD methods applied in this study are described hereafter.

### 3.2.1. The Delta change method

By assuming that the relative changes obtained from the GCMs are more representative than the absolute ones, the simple Delta method maintains the temporal structure of the projected series, hence does not consider changes in variability. The future daily rainfall ($P_{Fut,d}$) is obtained by multiplying the observed daily series ($P_{Obs,d}$) by the ratio of the mean monthly rainfall value for the GCM scenario series ($P_{Sce,m}$) to the control series ($P_{Con,m}$).

$$P_{Fut,d}[mm/day] = P_{Obs,d} \times \frac{P_{Sce,m}}{P_{Con,m}} \tag{3}$$

The advantages of the Delta method are:

- it is simple to apply
- it preserves the observed pattern of temporal and spatial variability

The disadvantages of the Delta method include the following:

- it only accounts for the changes in mean; this is done while ignoring other possible changes in the distribution of the variables
- changes in the length of dry or wet spells are not taken into consideration
- it is not suitable for extreme events
- it requires data to be normally distributed

### 3.2.2. Quantile perturbation method

In the quantile perturbation approach, the changes obtained from comparing the GCM scenario with control or historical series are considered dependent on the daily rainfall intensity (see e.g. Mpelasoka and Chiew, 2009; Willems and Vrac, 2011). In a number of studies including Chiew (2006), Harrold et al. (2005) and Harrold and Jones (2003), the quantile mapping method, which quantile perturbation approach makes use of, was used to scale ranked historical daily rainfall quantiles to establish future quantiles. Consider for a selected rainfall intensity threshold, e.g. >1 mm/day, the GCM scenario series quantiles denoted as $sx_1 \geq sx_2 \geq \ldots \geq sx_i \ldots \geq sx_B$; the GCM control series quantiles denoted as $cx_1 \geq cx_2 \geq \ldots \geq cx_i \ldots \geq cx_B$; the empirical quantiles as $ex_1 \geq ex_2 \geq \ldots \geq ex_i \ldots \geq ex_B$; and the quantile perturbation factors $Qp_1 \geq Qp_2 \geq \ldots \geq Qp_i \ldots \geq Qp_B$, the relative $Qp_i$ is calculated as $sx_i/cx_i$ where $i$ is the rainfall intensity rank ($i = 1$ for the highest; $i = B$ for the lowest intensity).

The advantages of this method are that:

- it considers correction of rainfall intensity frequency
- the sequences of the wet/dry days are preserved
- it is suitable for extreme events
- no assumptions about the nature of probabilities of events are required

The disadvantage of the quantile-based perturbation method include the following:

- based on the threshold selected, the valued for determining the perturbation factors (from the upper tail of the distribution) may be few
- similar correction is applied to all the months or seasons

#### 3.2.2.1. Simplified quantile perturbation.

The simplified quantile perturbation (simQP) method only considers changes in the daily rainfall intensities. Apart from the relative $Qp_i$ which are applied to rainfall intensities ≥ 1 mm/day, the absolute changes $|sx_i - cx_i|$ are considered for intensities lower than 1 mm/day. This approach was applied by Mora et al. (2014). The rationale for considering absolute for low rainfall intensities is twofold; first, to circumvent the amplification of resulting factors in the case $cx_i$ is close to zero; second, multiplying very small values of $ex_i$ by whatever $Qp_i$ yields very small resulting figures. The latter situation would not be so meaningful when the focus is on rainfall high extremes. The daily quantile based on $Qp_i$ are obtained for each of the twelve months and later on applied for the generation of future series. The simQP is calculated using Eqs. (4) and (5).

$$P_{Fut}(i)[mm/day] = ex_i \times \frac{sx_i}{cx_i} \text{ for rainfall intensity} \geq 1 \text{ mm/day} \tag{4}$$

$$P_{Fut}(i)[mm/day] = ex_i + |sx_i - cx_i| \text{ for rainfall intensity} < 1 \text{ mm/day} \tag{5}$$

In this study, since the observed series were of record lengths greater than those of the scenarios, interpolation for the quantiles was done where necessary.

#### 3.2.2.2. Advanced quantile perturbation.

This more advanced quantile perturbation method (wetQP) considers changes in both wet-day rainfall intensity and the frequency (Ntegeka et al., 2014; Nyeko-Ogiramoi et al., 2012b; Willems and Vrac, 2011). The procedure of the wetQP applied in this study was adopted from Nyeko-Ogiramoi et al. (2012b) (where details on the method can be found) and involves the following seven steps (applied to each of the 12 months).

(1) Select a threshold intensity that defines a wet day from observed, control and scenario series.
(2) Calculate the relative $Qp_i$ depending on the wet-day intensities.
(3) Apply to each of the wet-day intensities in the historical time series the $Qp_i$ using Eq. (4).
(4) Calculate the change factor on the wet-day frequency.
(5) Extend or reduce the length of the wet spells according to the wet-day frequency change factor.
(6) Calculate the new climate change signal at local scale after application of the wet-spell perturbation and validate it against the $Qp_i$ obtained in step (2). The validation of results is done through graphical comparison based on: (i) mean monthly volume of the wet-day intensity,

Please cite this article in press as: C. Onyutha, H. Tabari, A. Rutkowska, P. Nyeko-Ogiramoi, P. Willems, Comparison of different statistical downscaling methods for climate change rainfall projections over the Lake Victoria basin considering CMIP3 and CMIP5, Journal of Hydro-environment Research (2016), doi: 10.1016/j.jher.2016.03.001

(ii) mean wet-day daily intensity, (iii) mean wet spell and, (iv) coefficient of variation of the wet-day intensity.

(7) If the errors between the climate change signals in steps (6) and (2) are small enough based on closeness of the validation plots, then the perturbed observed series obtained in step (5) are the future projections, if not, repeat step (5)–(7).

### 3.3. Change in rainfall extremes

The current and projected rainfall intensity quantiles and totals after statistically downscaling of the GCM runs were compared to assess the impact of climate change. For the rainfall quantiles, Ts of 10, 5, 2 and 1.25 years were considered. This range of Ts is covered by a number of relevant water engineering or management applications. The change in the T-year event was assessed as the ratio of the difference ($x_g - x_e$) to $x_e$. Considering $d_{\text{obs}}$ ($d_{\text{fut}}$) as the observed (scenario) annual rainfall total, and $d_{\text{emp,z}}$ ($d_{\text{fut,z}}$) the observed (future) rainfall total for season $z$, changes in the annual rainfall was calculated as the difference ($d_{\text{fut}} - d_{\text{obs}}$) over $d_{\text{obs}}$. Correspondingly, the ratio of the difference ($d_{\text{fut,z}} - d_{\text{emp,z}}$) to $d_{\text{emp,z}}$ was used to assess changes in the rainfall total of $z$. Apart from the ensemble mean of the changes, also the Minimum (Min) and Maximum (Max) projections were obtained to assess the low and high scenarios for the quantiles of both the CMIP3 and CMIP5.

## 4. Results and discussion

### 4.1. Inter-GCM differences in reproducing rainfall extremes

Fig. 4 shows for stations 7, 1, 8 and 6 the observed quantiles versus those of the GCM control or historical simulations. For the CMIP3, the GCM runs with the slopes of their Ts clearly steeper than that of the empirical quantiles include CM3.0_R1, R1 of the CGT63, and R1 to R3 of the CGT47 (Fig. 4a). Such mismatches between the GCM-based and empirical quantiles can lead to higher values of the *Bias* and *SEE*. The GCMs of the CMIP5 (Fig. 4b, d, f and h) are shown to capture the observed rainfall extremes better than those of the CMIP3 (Fig. 4a, c, e and g). For the purpose of illustration, the measures of the deviation of $x_g$ for $x_e$ for the same quantiles and station shown in Fig. 4a and b are presented in Fig. 5a and b respectively.

For the CMIP3, two GCMs including CM2.0_R1 and CM2.1_R1 are shown to project comparatively higher absolute amount of variabilty in the future rainfall extremes than others. At the rainfall stations 1–9, the *Biases* of CM2.1_R1 were all negative and greater than 100% in magnitude. This same observation was also noted for the *Biases* of CM2.0_R1 at stations 1–6. The values of the *Bias* of CM2.0_R1 at stations 7–9 were −44.7, −72.2 and −96.4% respectively. At station 9, poor performance was exhibited by MK3.0_R1 and MK3.5_R1 with bias 118% and 156% respectively. On the other hand, top performance (low *Bias*) were produced by R1 and R2 of MI3.2M (at stations 2–5 and 8–9), R1 and R4 of ECH5 (at stations 1 and 6), and R2 and R3 of ECHO-G (at stations 7). The *biases* of MI3.2M (R1, R2) at station 2–5 and 8–9 were (18.6, 18.2%), (−15.5, −7.7%), (−2.9, 1.7%), (12.1, 5.1%), (20.1, 19.4%), and (9.8, 13.4%) respectively. For the CMIP5, the GCM runs with top performance included MMR_R1 (at station 1, bias of −1.1%), BNU_R1 (at stations 2 and 7 with bias of −3.2 and −2.3% respectively), GFCM_R1 (at stations 3 and 8 with bias of 4.2 and 2.9% respectively), GFCM_R3 (at stations 5–6 with bias of 5.1 and 1.1% respectively), and MK3.6_R8 (at station 9 with bias of −8.8%). Poor performance (with *Bias* mostly above 10%) was exhibited by BNU_R1 (at stations 1, 3, 4–5, and 9), and MLR_R1 (at stations 2, 4, 6–7 and 8).

Based on the ensemble mean of *Bias* and *SEE*, it is shown in Fig. 6 that the CMIP5 performed better than the CMIP3 in reproducing the rainfall extremes. The ensemble mean of *Bias* for the CMIP5 varies from −19.05% (station 5) to 3.11% (station 7). Correspondingly, values of −65.85% (station 4) to −4.86% (station 7) were obtained for the CMIP3. This smaller values of the *Bias* and *SEE* for the CMIP5 than those of the CMIP3 reflect the improvement of the newer generation GCMs hence the improved applicability of those GCMs to cope with the data quality of the LVB. Regardless of the magnitude of the bias, from Fig. 6a it can be noted that the stations with low values of the ensemble *Bias* in the CMIP3 also yield low values in the CMIP5. At some stations, values of the ensemble *Bias* are high for both the CMIP3 and CMIP5. This suggests that there is some similarity in the pattern (but not the magnitude) of the rainfall intensity extremes in both the CMIP3 and CMIP5. The performance of the GCM simulations to capture the rainfall extremes, however, varies from station to station. This is not suprising given the high spatial difference in the variability of rainfall across the study area. Previous studies on spatial difference of some statistics including the rainfall totals (Onyutha and Willems, 2015b) and extreme intensities (Nyeko-Ogiramoi et al., 2012a) for the NEQ are higher than for other parts of the LVB. It was shown by Onyutha and Willems (2015a) that the temporal pattern of rainfall variability in the stations in the NEQ (3 and 9) is different from the rest of other parts of the LVB. This could bring about the spatial difference in the rainfall extreme intensities across the study area. Higher temporal variability could be because of stronger difference between short-duration and longer duration values or stronger differences between low and high extreme events (Onyutha and Willems, 2015b).

### 4.2. Differences in the outcomes of the SD methods for patterns of monthly rainfall

Fig. 7 shows, for the purpose of illustration using station 8, the patterns of the monthly rainfall totals in the observed versus those of the GCMs for the 2050's high scenario A2 (rcp8.5) of the CMIP3 (CMIP5). The figure also shows the difference in the influences of the different SD methods on the rainfall totals. Before the downscaling procedure, closer match in the bimodal rainfall pattern is obtained using the GCMs of the CMIP5 (Fig. 7e) than those of the CMIP3 (Fig. 7a). However, for most of the GCMs of the CMIP5 (Fig. 7e), there are more overestimations in the OND rainfall than for the MAM rainy season. This overestimation by the GCMs could be due to the difficulty to capture the variations in the 'short' rains (OND) which is known to be more dominant than that of the MAM rainfall in the study area (Nicholson, 1996). The differences between the



Please cite this article in press as: C. Onyutha, H. Tabari, A. Rutkowska, P. Nyeko-Ogiramoi, P. Willems, Comparison of different statistical downscaling methods for climate change rainfall projections over the Lake Victoria basin considering CMIP3 and CMIP5, Journal of Hydro-environment Research (2016), doi: 10.1016/j.jher.2016.03.001

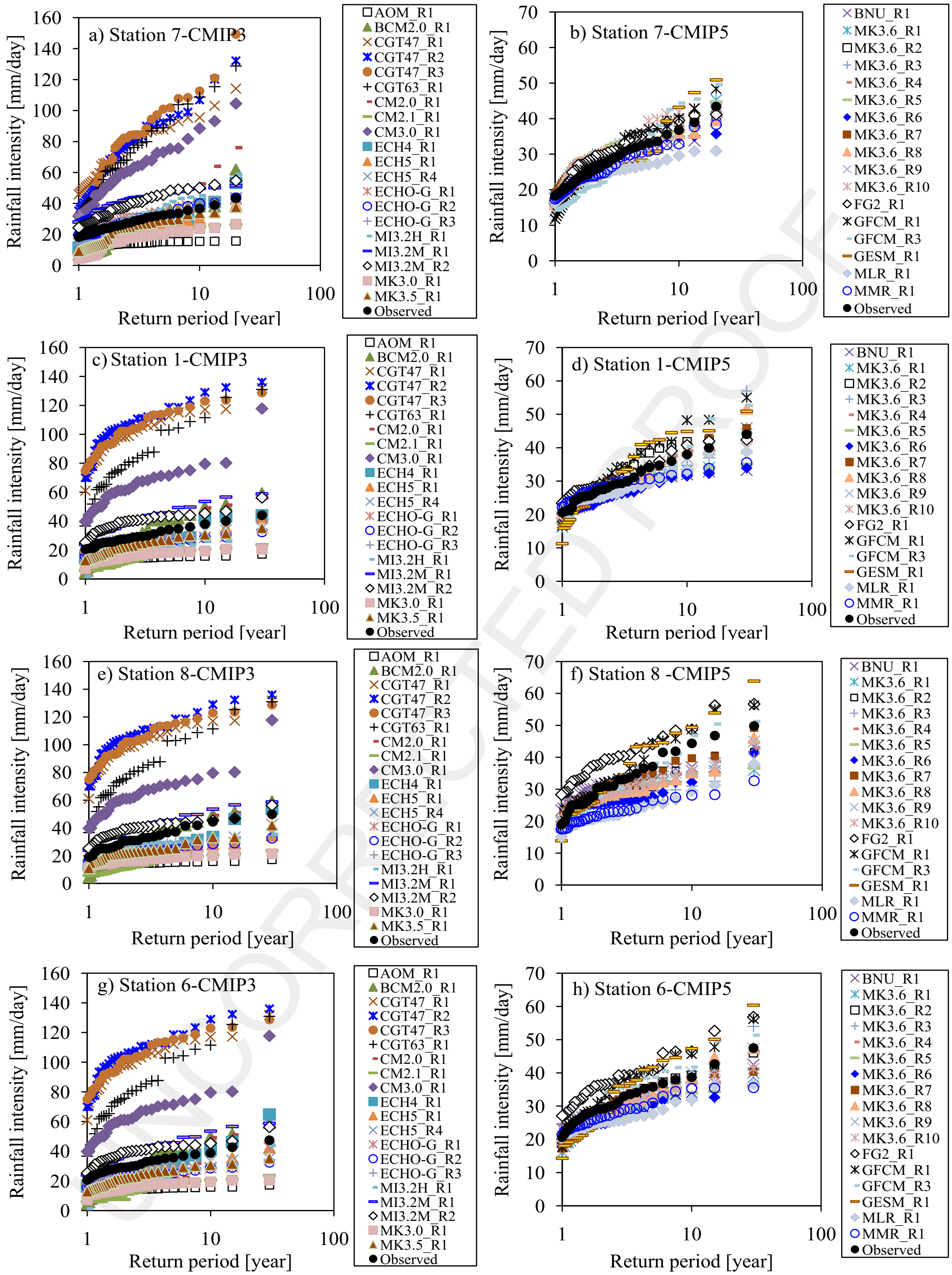


Fig. 4. Daily rainfall intensity quantiles versus empirical return period at (a–b) Station 7, (c–d) Station 1, (e–f) Station 8, and (g–h) Station 6. The charts (a), (c), (e), and (g) are for the CMIP3, and (b), (d), (f), and (h) for CMIP5.

patterns of the downscaled totals for the three SD methods are not significant (Fig. 7a–h). It can be noted that, on average, the downscaled outputs of the GCMs in the CMIP3 are generally higher than those of the CMIP5. This could suggest that the projections of the rainfall totals for the GCMs of the CMIP3 may be higher than those of the CMIP5. Generally for the Delta and simQP, the outputs from the GCMs of the CMIP3 overestimate rainfall totals of the rainy (MAM and OND) seasons. Because the perturbation factors are used as multipliers for the empirical quantiles (for the simQP) and observed daily series (for the Delta), if they are high for the rainy seasons, they influence the overestimation of the long-term seasonal pattern



Please cite this article in press as: C. Onyutha, H. Tabari, A. Rutkowska, P. Nyeko-Ogiramoi, P. Willems, Comparison of different statistical downscaling methods for climate change rainfall projections over the Lake Victoria basin considering CMIP3 and CMIP5, Journal of Hydro-environment Research (2016), doi: 10.1016/j.jher.2016.03.001

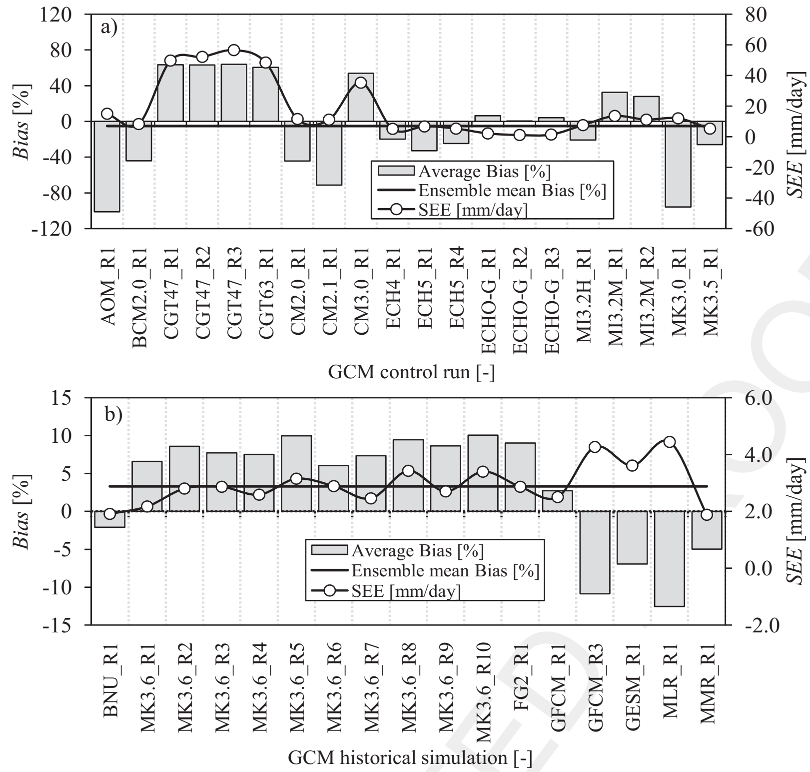


Fig. 5. *Bias* [%] and *SEE* [mm/day] of daily rainfall intensity quantiles at station 7 for (a) CMIP3 and (b) CMIP5.

of the GCM series compared with that of the observed rainfall. Question, however, remains on how realistic the perturbation factors are for the GCMs that do not capture the seasonality patterns well for the control runs.

Comparable performances of the GCMs in capturing the patterns of the monthly rainfall totals were obtained for stations 1–2, 4, and 6–8. However, for the NEQ of the LVB (stations 3, 5 and 9), the skill of the GCMs from both the CMIP3 and CMIP5 were low in capturing the pattern of the monthly rainfall. Although it was already seen in Fig. 3 that the July to September (JAS) period at stations (3, 5 and 9) is a wet season, the GCMs at these locations instead reproduced this JAS period as a dry one. Some question worth attempting to answer is why the rainfall pattern at stations 3 and 9 (also at 5 to some extent) is different from others. The rainfall of these stations may be indicative of the interacting influence of both the Mount Elgon and Lake Victoria in the region. The differences in regional features such as water bodies, transition in land cover and/or use, physiographic characteristics, e.g. topography, etc. can cause the patterns of variability over various parts of a basin to differ. It may also be possible that the low quality of the data at these stations in the NEQ could be responsible for the making its rainfall statistics (in terms of its monthly pattern as well as its variability) different from other parts of the LVB (Onyutha and Willems, 2015a). The poor performance of the GCMs in capturing the monthly pattern of the rainfall in the NEQ of the LVB is because the resolutions of the GCMs are coarse. For more realistic downscaling of rainfall in the NEQ of the LVB, GCMs of resolutions finer than those used in this study can be used. Alternatively, the capability of the Regional Climate Models (RCMs), e.g. those used in Coordinated Regional Climate Downscaling Experiment (CORDEX) to simulate

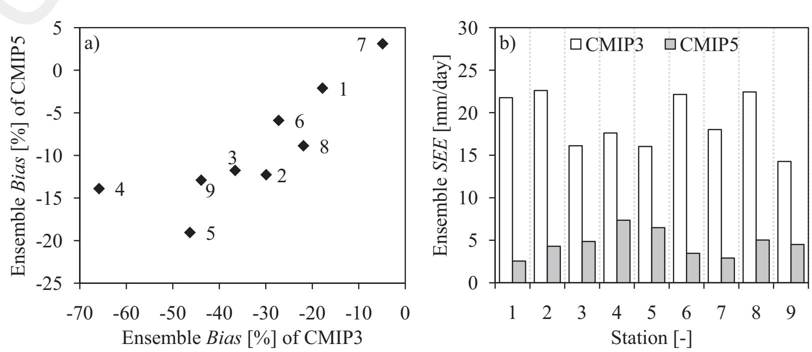


Fig. 6. (a) Ensemble *Bias* [%] and b) *SEE* [mm/day] of daily rainfall intensity quantiles at all the 9 stations; the data labels in chart (a) are the station numbers.

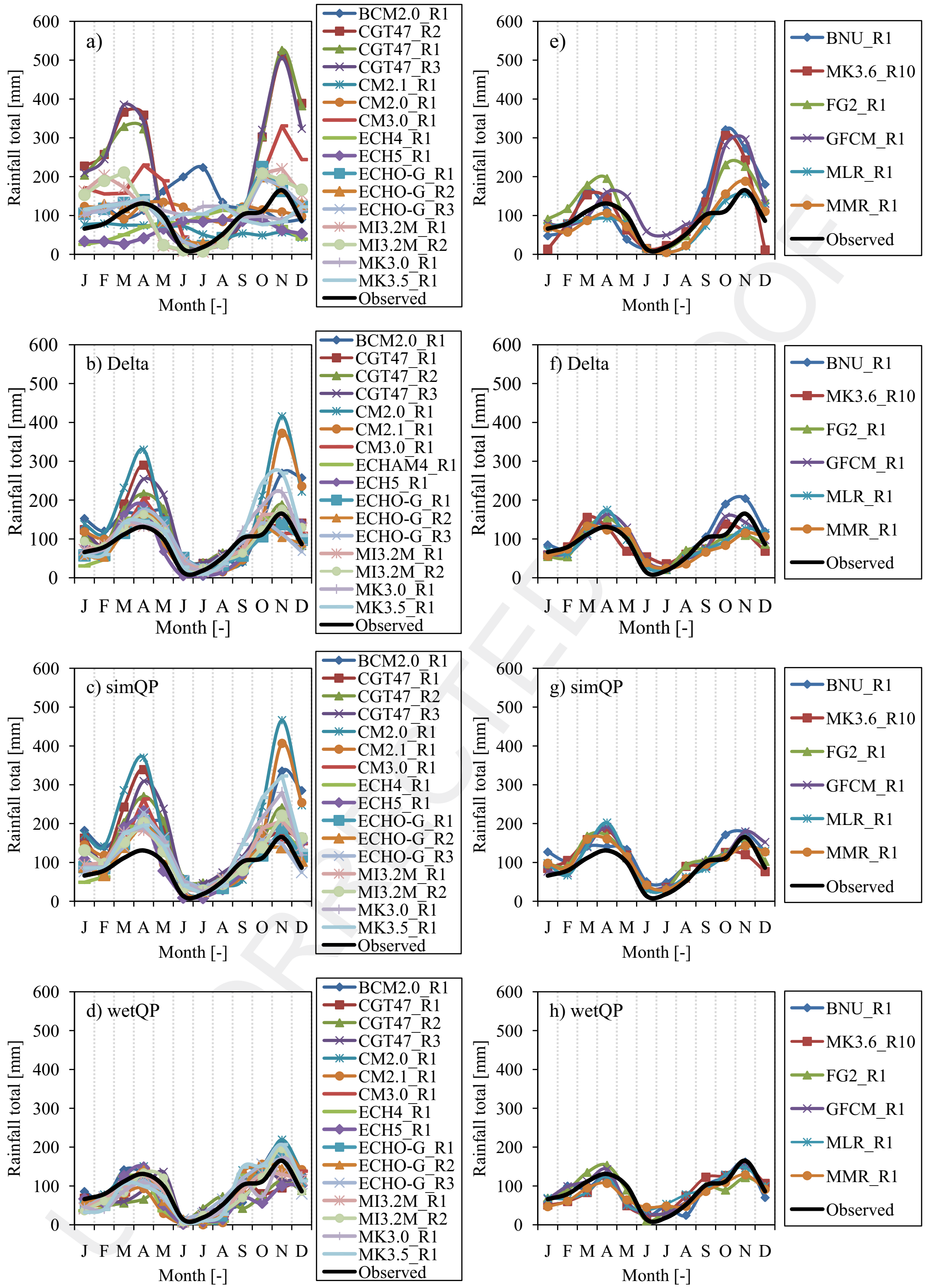


Fig. 7. Monthly rainfall totals at station 8 for (a–d) CMIP3, and (e–h) CMIP5. Charts for the scenarios before and after the SD are shown in (a, e) and (b–d, f–h), respectively.

the characteristics of rainfall pattern over the LVB can be assessed.

### 4.3. Changes in rainfall quantiles

Fig. 8 shows, for illustration, the changes in the rainfall intensity quantiles at station 1 for the selected Ts obtained by the different SD methods. It is noticeable that for Ts of 2.5, 5 and 10 years, the changes obtained are from the lowest to the highest for Delta, simQP and wetQP respectively (see Fig. 8a–f). The low projections of the future rainfall series obtained by the Delta method follow from the perturbation of the monthly mean rather than the individual daily quantiles.

Please cite this article in press as: C. Onyutha, H. Tabari, A. Rutkowska, P. Nyeko-Ogiramoi, P. Willems, Comparison of different statistical downscaling methods for climate change rainfall projections over the Lake Victoria basin considering CMIP3 and CMIP5, Journal of Hydro-environment Research (2016), doi: 10.1016/j.jher.2016.03.001

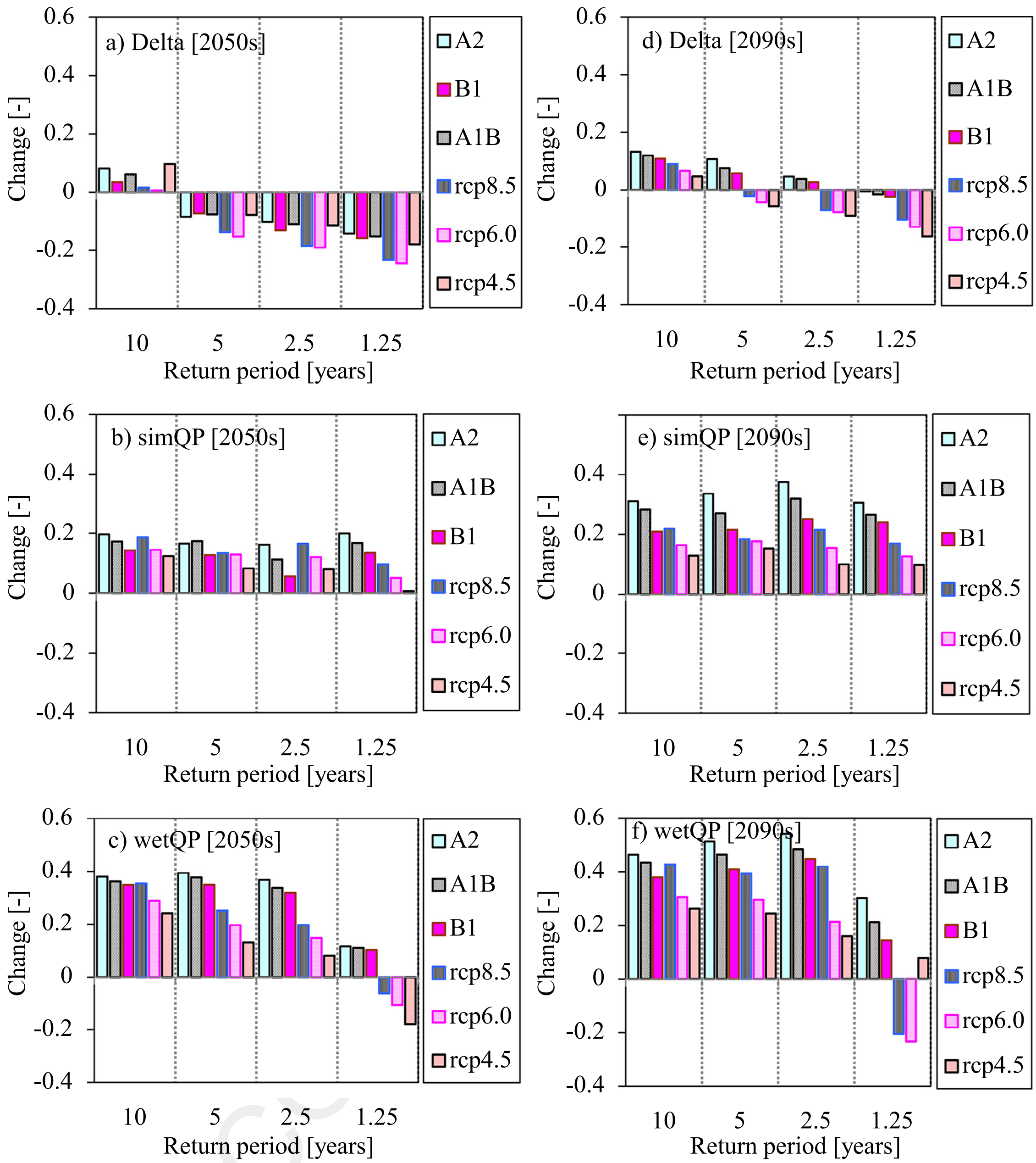


Fig. 8. Ensemble mean changes in rainfall intensity quantiles at station 1 for (a–c) 2050s, and (d–f) 2090s.

This indicates inadequacy of the Delta method for series with significant changes in variability under climate change. Therefore, caution should be taken when using the Delta downscaling method in studying rainfall extremes. It should be used alongside other more downscaling methods suitable for rainfall extremes. The higher changes in rainfall quantiles by the wetQP than other methods is due to strong differences in the length of wet spell and the magnitude of the rainfall quantiles derived from some control or historical and scenario runs. It can be noted that both the simQP and wetQP methods project positive changes in the rainfall quantiles. The rainfall projections obtained from the wetQP are higher than those of the simQP. If the accuracy of the projections can be ascribed to the considerations of the wet/dry spells as well as the intensity frequency, it means that the results from the wetQP are more reliable than those of the simQP. The difference between the simQP and wetQP is less than that of each of the quantile perturbation methods and the Delta method. This follows the fact that for period with low rainfall, the monthly mean of such intensities as considered by the Delta method can be far lower than for the extreme quantiles used in the simQP and wetQP approaches. The difference between the outcomes of the SD methods can partly be related to data scarcity and variability. This is because data of low quality can increase mismatch between observed rainfall intensity and GCM control simulations, thereby influencing the differences between the results of the SD methods.

Generally for the selected Ts, the changes projected by the GCMs of the CMIP5 (Fig. 8d–f) are slightly lower than those of

Please cite this article in press as: C. Onyutha, H. Tabari, A. Rutkowska, P. Nyeko-Ogiramoi, P. Willems, Comparison of different statistical downscaling methods for climate change rainfall projections over the Lake Victoria basin considering CMIP3 and CMIP5, Journal of Hydro-environment Research (2016), doi: 10.1016/j.jher.2016.03.001

Table 4
Minimum (min), average (mean) and maximum (max) changes [%] in 10-year rainfall quantile for the different downscaling methods.

| Scenario and time horizons | | | Delta | | | simQP | | | wetQP | | |
|---|---|---|---|---|---|---|---|---|---|---|---|
| | | | Min | Mean | Max | Min | Mean | Max | Min | Mean | Max |
| CMIP3 | 2050s | A2 | −7.3 | 11.7 | 50.3 | −17.0 | 15.9 | 71.4 | −17.0 | 43.6 | 117.9 |
| | | A1B | −21.4 | 10.2 | 45.1 | −24.3 | 14.2 | 62.0 | −25.2 | 32.0 | 102.3 |
| | | B1 | −48.2 | 8.4 | 37.5 | −31.3 | 12.0 | 72.1 | −40.3 | 20.4 | 89.1 |
| | 2090s | A2 | −13.3 | 14.2 | 63.0 | −19.8 | 23.3 | 62.6 | −18.0 | 40.6 | 107.3 |
| | | A1B | −11.4 | 13.4 | 47.8 | −22.0 | 19.1 | 78.2 | −20.4 | 35.9 | 103.2 |
| | | B1 | −21.2 | 12.2 | 40.4 | −30.9 | 14.8 | 73.0 | −27.2 | 30.4 | 95.1 |
| CMIP5 | 2050s | rcp8.5 | −19.8 | 5.8 | 39.5 | −24.3 | 10.0 | 65.9 | −50.6 | 22.4 | 170.5 |
| | | rcp6.0 | −23.9 | 4.2 | 33.1 | −30.7 | 6.5 | 50.0 | −50.8 | 16.6 | 112.0 |
| | | rcp4.5 | −46.7 | 3.1 | 30.6 | −42.4 | 5.8 | 46.6 | −51.6 | 11.2 | 78.3 |
| | 2090s | rcp8.5 | −30.0 | 8.0 | 40.7 | −24.1 | 11.4 | 42.2 | −39.1 | 25.4 | 94.9 |
| | | rcp6.0 | −37.5 | 6.2 | 42.9 | −25.7 | 9.1 | 39.4 | −44.5 | 22.6 | 87.1 |
| | | rcp4.5 | −55.4 | 5.3 | 18.4 | −27.3 | 7.3 | 37.9 | −54.7 | 20.7 | 62.9 |

the CMIP3 (Fig. 8a–c). However, considering all the stations across the study area, the comparative range of impact changes in high and low scenario for each of the SD methods are moderate as seen in Table 4. According to Akurut et al. (2014), increase in rainfall extremes over the Lake Victoria of the LVB is expected to go up to 40%. In comparison with other stations used in this study, it was noted that this is consistent with the results of stations 1 (Fig. 8f) and 6 based on the wetQP SD method. For stations 2, 4, and 7–8, projections were below 40%. However, for stations in the NEQ (3, 5, and 9) the projections go up to 46%.

### *4.4. Changes in seasonal and annual rainfall*

Fig. 9 shows the ensemble mean changes in the rainfall intensity totals for the main wet (MAM) season as well as for the annual time scale using the different SD methods. The range over which the changes in rainfall varied from one station to the next was narrower for the wetQP than those of the Delta and simQP SD methods. On average, the changes in the annual rainfall and that of the MAM season show increase. However, for the main dry (JJAS) season (though not shown for brevity), on average the rainfall totals is projected to decrease for both

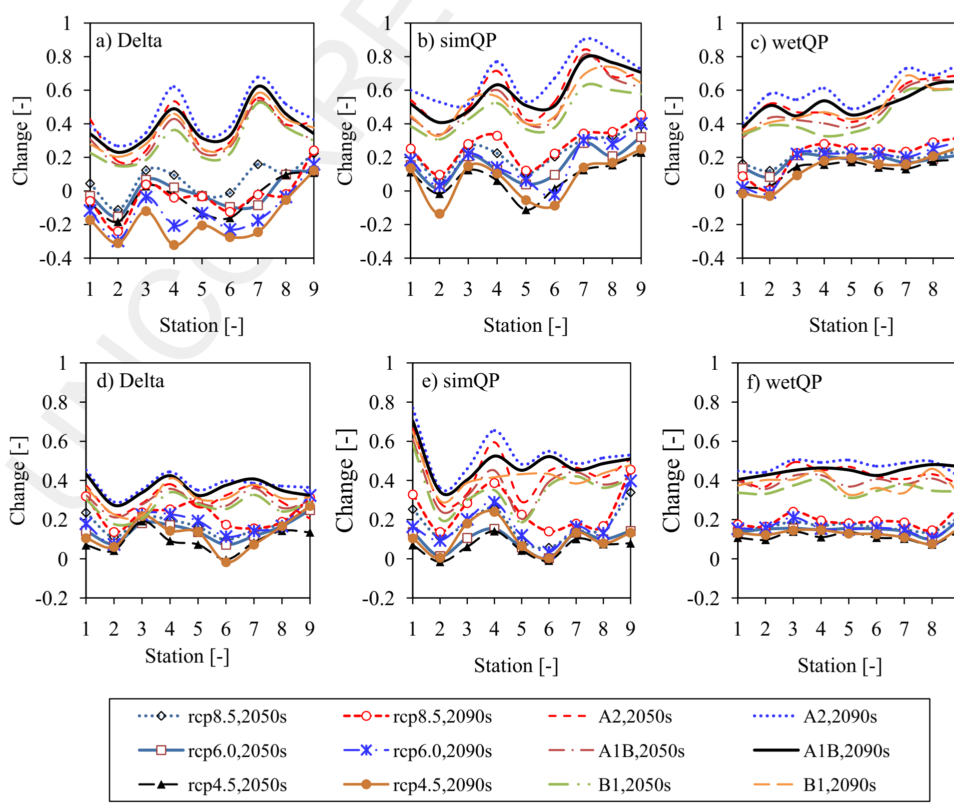


Fig. 9. Changes in rainfall totals for (a–c) MAM and (d–f) annual time scale. The legend is the same for all the charts; for each chart, the changes for the CMIP5 (CMIP3) are shown by lines or curves with (without) markers.



Please cite this article in press as: C. Onyutha, H. Tabari, A. Rutkowska, P. Nyeko-Ogiramoi, P. Willems, Comparison of different statistical downscaling methods for climate change rainfall projections over the Lake Victoria basin considering CMIP3 and CMIP5, Journal of Hydro-environment Research (2016), doi: 10.1016/j.jher.2016.03.001

the CMIP3 and CMIP5. This suggests that rainy and dry seasons will respectively become wetter and drier in the future (2050s and 2090s) than the conditions observed over the period 1961–2000. Considering separately the results of CMIP3 and CMIP5, the difference between the Delta and the quantile perturbation methods is smaller in projecting the seasonal and annual rainfall totals than for the changes in rainfall extremes.

It was noted that the projections for the rainfall totals by the GCMs of the CMIP5 were systematically lower than those of the CMIP3. However, for either the CMIP3 or CMIP5, the difference in projected changes in rainfall totals between the outputs of the different SD method was shown to be insignificant. These results are consistent with the explanations from Fig. 7. Using the CMIP5, the projection of annual rainfall over the study area by IPCC (2013) for the 2090s goes up to about 10%. According to Akurut et al. (2014), the total annual precipitation over the Lake Victoria (in the central part of the LVB) is expected to increase by less than 10% (for the rcp4.5) and less than 20% (for the rcp8.5). In this study, the projections, on average, for the annual rainfall over the 21st century obtained for the Delta, simQP and wetQP are 20.7, 21.6 and 18.1% (for the rcp8.5), 14.4, 13.5 and 12.4% (for the rcp6.0), and 11.0, 8.3 and 10.0% (for the rcp4.5) respectively. If not because of the ensemble mean, projected rainfall changes of some GCMs were noted to go higher than 100%. Exaggerated projections of the rainfall totals might stem from the mismatch between the observed seasonal or monthly rainfall and that of the GCM-based series before downscaling. In such a case, the GCM simulations that prove to be significantly inconsistent could be discarded and left out during the SD. In this study, however, no GCM run was discarded at any station because, on average, they performed moderately well in capturing the seasonal and monthly totals.

## 5. Conclusions

In transferring the climate signals to the observed rainfall for applications of design, operation and maintenance of risk based water resources systems, three SD methods including the Delta, the simQP and wetQP approaches were considered and compared. The inter-GCM differences in reproducing the rainfall extremes as well as the pattern of the monthly totals were assessed. The findings are summarized as follow:

- Because the outputs from the three SD methods captured well the pattern of monthly rainfall totals, the difference between the projected changes of seasonal or annual rainfall totals from the Delta, simQP and wetQP was shown to be insignificant.
- Generally, the magnitudes of the rainfall quantiles are projected to increase in the future as exhibited based on both the CMIP3 and CMIP5. However, the projected changes in the rainfall extremes from the CMIP5 were lower than those of the CMIP3. Rainfall totals of the wet (dry) season are projected to increase (decrease) in both the 2050s and 2090s. The changes for return periods of 2.5, 5 and 10 years were from the lowest to the highest obtained for Delta, simQP and wetQP respectively. If the assumption would be made that the wetQP method provides the most accurate change in the extreme quantiles, based on the CMIP3 (CMIP5) projections, the Delta and simQP underestimate these quantiles with about 29% and 23% (17% and 14%) respectively for the 10-year return period rainfall intensity quantile. These systematic difference in the results from the different SD methods indicate that the choice of the appropriate method can be made on a case by case basis in line with the objectives of the climate change impact study; e.g. the Delta does not capture well the changes in rainfall extremes, the wetQP is suitable for both rainfall extremes and rainfall totals at both seasonal and annual time scales. It moreover shows that next to the uncertainties in the greenhouse gas scenarios and climate model projections, there is important additional uncertainty in the SD. Although there is a need to conduct further studies on the accuracy of specific SD approaches, even after such studies it would remain difficult to select one SD approach as the best one. Consequently, an ensemble approach with several plausible SD methods, including other methods than the ones applied in this study, can be recommended.

## Acknowledgments

The research was financially supported by an IRO PhD scholarship of KU Leuven. The authors are thankful to the Editor-in-Chief Joseph H.W. Lee as well as the four anonymous reviewers for their constructive comments that greatly enhanced the quality of this paper.

## References

Akurut, M., Willems, P., Niwagaba, C.B., 2014. Potential impacts of climate change on precipitation over Lake Victoria, East Africa, in the 21st Century. Water 6, 2634–2659.

Artlert, K., Chaleeraktrakoon, C., Nguyen, V.-T.-V., 2013. Modeling and analysis of rainfall processes in the context of climate change for Mekong, Chi, and Mun River Basins (Thailand). J. Hydro. Environ. Res. 7 (1), 2–17.

Awange, J.L., Ong'ang'a, O., 2006. Lake Victoria: Ecology, Resources, Environment. Springer, Berlin, Germany. ISBN-13: 9783540325741, ISBN: 3540325743.

Beyene, T., Lettenmaier, D.P., Kabat, P., 2010. Hydrologic impacts of climate change on the Nile River basin: implications of the 2007 IPCC scenarios. Clim. Chang. 100, 433–461.

Bezak, N., Brilly, M., Šraj, M., 2014. Comparison between the peaks-over-threshold method and the annual maximum method for flood frequency analysis. Hydrol. Sci. J. 59 (5), 959–977.

Chen, J., Brissette, F.P., Leconte, R., 2011. Uncertainty of downscaling method in quantifying the impact of climate change in hydrology. J. Hydrol. 401 (3–4), 171–184.

Chiew, F.H.S., 2006. An overview of methods for estimating climate change impact on runoff. Paper presented at the 30th Hydrology and Water Resources Symposium, Lauceston, Australia, 4–7 December, CDROM [ISBN 0-8582579-0-4], Engineers Australia, Barton, Australian Capital Territory.

Conway, D., Hulme, M., 1996. The impacts of climate variability and future climate change in the Nile Basin on water resources in Egypt. Int. J. Water Resour. Develop. 12, 277–296.

DDC, 2015. What is a GCM? <http://www.ipcc-data.org/guidelines/pages/gcm_guide.html> (accessed 17.04.15.).

Dessu, S.B., Melesse, A.M., 2013. Evaluation and comparison of satellite and GCM rainfall estimates for the Mara River Basin, Kenya/Tanzania. In: Younos, T., Grady, C.A. (Eds.), Climate Change and Water Resources. The

Handbook of Environmental Chemistry. Springer-Verlag Berlin Heidelberg, vol. 25. pp. 29–45. doi:10.1007/698_2013_219.

Fathelrahman, E., Davies, A., Davies, S., Pritchett, J., 2014. Assessing climate change impacts on water resources and Colorado agriculture using an equilibrium displacement mathematical programming model. Water 6 (6), 1745–1770.

Fiddes, D., Forsgate, J.A., Grigg, A.O., 1974. The prediction of storm rainfall in East Africa. Transport and Road Research Laboratory (TRRL) report 623, Environment Division of Transport Systems Department, TRRL, Crowthorne, Berkshire, 25pp.

Fowler, H.J., Blenkinsop, S., Tebaldi, C., 2007. Linking climate change modelling to impacts studies: recent advances in downscaling techniques for hydrological modelling. Int. J. Climatol. 27, 1547–1578.

Ghosh, S., Katkar, S., 2012. Modeling uncertainty resulting from multiple downscaling methods in assessing hydrological impacts of climate change. Water Resour. Manage. 26, 3559–3579.

Githui, F., Gitau, W., Mutua, F., Bauwens, W., 2009. Climate change impact on SWAT simulated streamflow in western Kenya. Int. J. Climatol. 29, 1823–1834.

Harrold, T.I., Jones, R.N., 2003. Downscaling GCM rainfall: a refinement of the perturbation method. Paper presented at International Congress on Modelling and Simulation (MODSIM 2003), Townsville, 14–17 July, Modelling and Simulation Society of Australia and New Zealand, Canberra, Australia.

Harrold, T.I., Chiew, F.H.S., Siriwardena, L., 2005. A method for estimating climate change impacts on mean and extreme rainfall and runoff. In: Zerger, A., Argent, R.M. (Eds.), MODSIM 2005 International Congress on Modelling and Simulation. Modelling and Simulation Society of Australia and New Zealand, Melbourne; Victoria, Australia, pp. 497–504.

IPCC, 2001. Climate Change: The Scientific Basis. Cambridge University Press, Cambridge and New York, NY, USA, p. 996.

IPCC, 2012. Managing the Risks of Extreme Events and Disasters to Advance Climate Change Adaptation. A Special Report of Working Groups I and II on the IPCC. Field, C.B., Barros, V., Stocker, T.F., Qin, D., Dokken, D.J., Ebi, K.L., et al. (Eds.). Cambridge University Press, Cambridge, UK, and New York, NY, USA. 582 pp.

IPCC, 2013. Climate Change 2013: The Physical Science Basis. Contribution of Working Group I to the Fifth Assessment Report of the IPCC. Cambridge University Press, Cambridge, United Kingdom and New York, USA. 1535pp.

Khan, M.S., Coulibaly, P., Yonas Dibike, Y., 2006. Uncertainty analysis of statistical downscaling methods. J. Hydrol. 319, 357–382.

Kizza, M., Rodhe, A., Xu, C.-Y., Ntale, H.K., 2011. Modelling catchment inflows into Lake Victoria: uncertainties in rainfall–runoff modelling for the Nzoia River. Hydrol. Sci. J. 56 (7), 1210–1226.

Kizza, M., Guerrero, J.-L., Rodhe, A., Xu, C.-Y., Ntale, H.K., 2013. Modelling catchment inflows into Lake Victoria: regionalisation of the parameters of a conceptual water balance model. Hydrol. Res. 44 (5), 789–808.

Knutti, R., Sedlácek, J., 2012. Robustness and uncertainties in the new CMIP5 climate model projections. Nat. Clim. Chang. doi:10.1038/NCLIMATE1716.

Kumar, D., Kodra, E., Ganguly, A.R., 2014. Regional and seasonal intercomparison of CMIP3 and CMIP5 climate model ensembles for temperature and precipitation. Clim. Dyn. 43, 2491–2518. http://dx.doi.org/10.1007/s00382-014-2070-3.

Lee, A., Cho, S., Kang, D.K., Kim, S., 2014. Analysis of the effect of climate change on the Nakdong river stream flow using indicators of hydrological alteration. J. Hydro. Environ. Res. 8 (3), 234–247.

Maraun, D., Wetterhall, F., Ireson, A.M., Chandler, R.E., Kendon, E.J., Widmann, M., et al., 2010. Precipitation downscaling under climate change. Recent developments to bridge the gap between dynamical models and the end user. Rev. Geophys. 48, RG3003. doi:10.1029/2009RG000314.

Meehl, G.A., Covey, C., Delworth, T., Latif, M., Mcavaney, B., Mitchell, J.F.B., et al., 2007. The WCRP CMIP3 multimodel dataset climate change research: a new era in climate change reserach. Bull. Amer. Meteor. Soc. 88, 1382–1394.

Melesse, A.M., Bekele, S., McCornick, P., 2011. Introduction: hydrology of the Nile in the face of climate and land-use dynamics. In: Melesse, A.M. (Ed.), Nile River Basin: Hydrology, Climate and Water Use. Springer, Dordecht, the Netherlands, pp. vii–xvii.

Mora, D.E., Campozano, L., Cisneros, F., Wyseure, G., Willems, P., 2014. Climate change of hydrometeorological and hydrological extremes in the Paute basin. Ecuadorean Andes. Hydrol. Earth Syst. Sci. 18, 631–648.

Mpelasoka, F.S., Chiew, F.H.S., 2009. Influence of rainfall scenario construction methods on runoff projections. J. Hydrometeorol. 10, 1168–1183.

Nakicenovic, N., Alcamo, J., Davis, G., de Vries, B., Fenhann, J., Gaffin, S., et al., 2000. Special Report on Emissions Scenarios: A Special Report of Working Group III of the Intergovernmental Panel on Climate Change. Cambridge University Press, Cambridge, UK. 599 pp. <http://www.grida.no/climate/ipcc/emission/index.htm>.

Nicholson, S.E., 1996. A review of climate dynamics and climate variability in Eastern Africa. In: Johnson, T.C., Odada, E.O. (Eds.), The Limnology, Climatology and Paleoclimatology of the East African Lakes. Gordon and Breach, Amsterdam, the Netherlands, pp. 25–56.

Nkomozepi, T., Chung, S.-O., 2014. The effects of climate change on the water resources of the Geumho River Basin, Republic of Korea. J. Hydro. Environ. Res. 8 (4), 358–366.

Ntegeka, V., Baguis, P., Roulin, E., Willems, P., 2014. Developing tailored climate change scenarios for hydrological impact assessments. J. Hydrol. 508C, 307–321.

Nyeko-Ogiramoi, P., Ngirane-Katashaya, G., Willems, P., Ntegeka, V., 2010. Evaluation and inter-comparison of Global Climate Models' performance over Katonga and Ruizi catchments in Lake Victoria basin. Phys. Chem. Earth 35, 618–633.

Nyeko-Ogiramoi, P., Willems, P., Mutua, F., Moges, S.A., 2012a. An elusive search for regional flood frequency estimates in the River Nile basin. Hydrol. Earth Syst. Sci. 16, 3149–3163.

Nyeko-Ogiramoi, P., Willems, P., Ngirane-Katashaya, G., Ntegeka, V., 2012b. Nonparametric statistical downscaling of precipitation from global climate models. In: Druyan, L. (Ed.), Climate Models. InTech Europe, University Campus STeP Ri. Slavka Krautzeka, Croatia, pp. 109–136. ISBN: 978-953-51-0135-2.

Onyutha, C., Willems, P., 2013. Uncertainties in flow-duration-frequency relationships of high and low flow extremes in Lake Victoria basin. Water 5 (4), 1561–1579.

Onyutha, C., Willems, P., 2015a. Uncertainty in calibrating generalised Pareto distribution to rainfall extremes in Lake Victoria Basin. Hydrol. Res. 46 (3), 356–376.

Onyutha, C., Willems, P., 2015b. Empirical statistical characterization and regionalization of amplitude-duration-frequency curves for extreme peak flows in the Lake Victoria Basin, East Africa. Hydrol. Sci. J. 60 (6), 997–1012.

Prudhomme, C., Davies, H., 2009. Assessing uncertainties in climate change impact analyses on the river flow regimes in the UK. Part 2: future climate. Clim. Chang 93, 197–222.

Prudhomme, C., Reynard, N., Crooks, S., 2002. Downscaling of global climate models for flood frequency analysis: where are we now? Hydrol. Process. 16, 1137–1150.

Quintana-Segui, P., Ribes, A., Martin, E., Habets, F., Boé, J., 2010. Comparison of three downscaling methods in simulating the impact of climate change on the hydrology of Mediterranean basins. J. Hydrol. 383, 111–124.

Taye, M.T., Ntegeka, V., Ogiramoi, N.P., Willems, P., 2011. Assessment of climate change impact on hydrological extremes in two source regions of the Nile River Basin. Hydrol. Earth Syst. Sci. 15, 209–222.

Taylor, K.E., Stouffer, R.J., Meehl, G.A., 2012. An overview of CMIP5 and the experiment design. B. Am. Meteorol. Soc. 93, 485–498. doi:10.1175/BAMS-D-11-00094.1.

Tungaraz, C., Eliapenda, E., Osewe, K.O., Palapala, P.M., 2012. Long-term climate impact on the Lake Victoria region influences water level fluctuation and resource availability. Int. J. Environ. Sci. 2, 1717–1732.

UNESCO, 2014. The FRIEND/Nile project. <http://www.unesco.org/new/en/cairo/naturalsciences/hydrology-programme/friendnile/> (accessed 02.01.14.).

Willems, P., Vrac, M., 2011. Statistical precipitation downscaling for small-scale hydrological impact investigations of climate change. J. Hydrol. 402, 193–205.



Please cite this article in press as: C. Onyutha, H. Tabari, A. Rutkowska, P. Nyeko-Ogiramoi, P. Willems, Comparison of different statistical downscaling methods for climate change rainfall projections over the Lake Victoria basin considering CMIP3 and CMIP5, Journal of Hydro-environment Research (2016), doi: 10.1016/j.jher.2016.03.001